TU Delft

Delft University of Technology

Nature of the Surface Intermediates Formed from Methane on Cu-ZSM-5 Zeolite

A Combined Solid-State Nuclear Magnetic Resonance and Density Functional Theory Study

Kolganov, Alexander A.; Gabrienko, Anton A.; Yashnik, Svetlana A.; Pidko, Evgeny A.; Stepanov, Alexander G.

DOI
10.1021/acs.jpcc.0c00311

Publication date
2020

Document Version
Accepted author manuscript

Published in
ACS Applied Materials and Interfaces

Citation (APA)
Kolganov, A. A., Gabrienko, A. A., Yashnik, S. A., Pidko, E. A., & Stepanov, A. G. (2020). Nature of the Surface Intermediates Formed from Methane on Cu-ZSM-5 Zeolite: A Combined Solid-State Nuclear Magnetic Resonance and Density Functional Theory Study. *ACS Applied Materials and Interfaces*, *124*(11), 6242-6252. https://doi.org/10.1021/acs.jpcc.0c00311

Important note
To cite this publication, please use the final published version (if applicable).
Please check the document version above.

Copyright
Other than for strictly personal use, it is not permitted to download, forward or distribute the text or part of it, without the consent of the author(s) and/or copyright holder(s), unless the work is under an open content license such as Creative Commons.

Takedown policy
Please contact us and provide details if you believe this document breaches copyrights.
We will remove access to the work immediately and investigate your claim.

This work is downloaded from Delft University of Technology.
For technical reasons the number of authors shown on this cover page is limited to a maximum of 10.

The Nature of the Surface Intermediates Formed from Methane on Cu-ZSM-5 Zeolite: A Combined Solid-State NMR and DFT Study

Alexander A. Kolganov,[1] *Anton A. Gabrienko*,[1,2] *Svetlana A. Yashnik*,[1]

Evgeny A. Pidko,[3,*] *Alexander G. Stepanov*[1,2,*]

[1]Boreskov Institute of Catalysis, Siberian Branch of the Russian Academy of Sciences, Prospekt Akademika Lavrentieva 5, Novosibirsk 630090, Russia

[2]Faculty of Natural Sciences, Department of Physical Chemistry, Novosibirsk State University, Pirogova Str. 2, Novosibirsk 630090, Russia

[3]Inorganic Systems Engineering group, Department of Chemical Engineering, Faculty of Applied Sciences, Delft University of Technology, Van der Maasweg 9, Delft 2629 HZ, The Netherlands

*e-mail: E.A.Pidko@tudelft.nl; stepanov@catalysis.ru

Abstract

The intermediates formed upon the interaction of methane with Cu-modified ZSM-5 zeolites (Cu/H-ZSM-5) have been analyzed with solid-state NMR spectroscopy and DFT methods. Methane activation by Cu/H-ZSM-5 zeolites gives rise to three distinct surface methoxy-like species (–O–CH_3) detected by ^{13}C MAS NMR spectroscopy with specific chemical shifts in the range of 53–63 ppm. DFT calculations on representative cluster models of different sites potentially present in Cu/H-ZSM-5 have been used to assign these signals to (i) methanol adsorbed on two neighboring Cu sites (Cu–($HOCH_3$)–Cu, 62.6 ppm), (ii) methanol adsorbed on zeolite Brønsted acid site (52.9 ppm) and (iii) lattice-bound methoxy groups (Si–O(CH_3)–Al, 58.6). The formation of these methoxy-like intermediates depends on the Cu loading and, accordingly, the type of Cu species in Cu/H-ZSM-5 zeolite. For the sample with low (0.1 wt.%) Cu loading containing exclusively mononuclear isolated Cu species, only the intermediates (ii) and (iii) have been detected. The Cu-bound intermediate (i) is formed upon methane activation by multinuclear Cu sites featuring Cu–O–Cu bridging moieties present in the materials with relatively higher Cu loading (1.38 wt.%). The presented results indicate

that methane activation by Cu/H-ZSM-5 can be promoted by both mono- and multinuclear Cu species confined in the zeolite matrix.

1. Introduction

Rising demand on the petrochemicals and limited crude oil reserves force the search for alternative feedstocks to produce valuable compounds. Methane, being major component of natural gas, is cheap and widely accessible raw material.[1] The conversion of methane to higher hydrocarbons or oxygenates over zeolite-based catalysts has attracted a considerable attention of the scientific community as a basis for future efficient gas-to-liquid technologies.[2-12] Despite great potential of methane as the feedstock for chemical industry, there are several important challenges hampering the efficient chemical processing of methane to such versatile chemical intermediates as, for example, methanol.[13] The key challenges are related to the low intrinsic reactivity of methane in combination with higher reactivity of the products of its conversion. In the context of oxidative conversion of methane, the desired products such as methanol and formaldehyde are much more susceptible to oxidation than methane resulting in severe loss of selectivity. Despite substantial efforts of both the academic and industrial research communities, the one-pot selective methane oxidation process that would be highly preferable in industry for the valorization of small-scale natural gas reserves has not been realized yet. The current indirect process involving the high-temperature methane conversion to syngas is highly energy and capital intensive.[14] The search for alternative efficient ways to convert methane to valuable chemicals, such as methanol, formaldehyde, acetic acid and various aromatic compounds, is an important challenge for contemporary catalysis science.[15-16]

Among different potential catalytic systems, Cu-containing zeolites have attracted a particular attention for selective oxo-functionalization of methane.[12, 17] The first attempts to use this type of catalysts for methane partial oxidation were inspired by some similarities between Cu-modified zeolites and methane monooxygenase (MMO), the enzyme which can perform methane-to-methanol conversion at ambient temperature.[18-19] In 2005, Groothaert et al.[20] discovered the ability of Cu-modified ZSM-5 and MOR zeolites to convert methane to methanol at a relatively low temperature of 398 K. It was suggested that $[Cu_2(\mu\text{-}O)_2]^{2+}$ core was the active site for the reaction. Later, the nature of the active site in Cu-ZSM-5 zeolites was revised on the basis of the results of Raman spectroscopy and density functional theory (DFT) calculations, and a $[Cu_2(\mu\text{-}O)]^{2+}$ species was proposed to be responsible for the low-temperature methane oxidation.[21] More recently, alternative active site proposals on the role

of trinuclear ($[Cu_3(\mu\text{-}O)_3]^{2+}$)[22-23] and mononuclear ($[Cu\text{-}OH]^{+}$)[24] active species have been put forward. Kinetic experiments on the isotope effect have shown that C–H cleavage is the limiting step of the methane conversion mechanism.[21] Quite a few works have been published on the influence of the structure of the active site,[23, 25] zeolite confinement,[26] and water addition[27-28] on the efficiency of methane activation on Cu-containing zeolites. However, there is still lack of experimental data on the nature of the surface intermediates formed upon methane activation by Cu/H-ZSM-5 zeolites.

High-resolution solid-state NMR technique is a powerful tool to clarify the pathways of methane activation mechanism on metal-containing zeolites.[2, 5, 7-8, 10, 29-37] ^{13}C MAS NMR spectroscopy can be fruitfully applied to inquire into the properties of Cu-loaded zeolites with respect to methane-to-methanol conversion. The approach is based on the analysis of ^{13}C MAS NMR spectra of methane adsorbed on the zeolite: the number of signals detected, the chemical shifts and the intensity of the signals. However, the assignment of the signals based on the observed chemical shifts is not straightforward in some cases.

So far, few works have been reported on the utilization of the ^{13}C MAS NMR method to study methane activation by Cu-containing MOR and ZSM-5 materials.[38-41] The signals with specific chemical shifts of various methoxy species (52–67 ppm) were observed in the ^{13}C MAS NMR spectra. Three signals at 61, 56 and 53 ppm were observed for Cu-MOR, which were assigned to Cu–O(CH_3)–Cu, Si–O(CH_3)–Al and adsorbed methanol molecules.[38] For Cu-ZSM-5, methane activation gave rise to two signals at 59 ppm and 53 ppm, attributed to Cu–OCH_3 and the adsorbed methanol, respectively.[40]

Two recent works[39, 41] have reported similar results from a combined ^{13}C MAS NMR and FTIR study on the nature of methoxy-like intermediates formed upon methane activation by Cu-MOR. In both cases, the signals at 58–59 ppm and at 50–54 ppm were detected and they were assigned to Si–O(CH_3)–Al species and methanol adsorbed on Brønsted acid sites (BAS), respectively. The formation of the signal at 62 ppm was detected only in one of the studies,[39] and it was assumed to correspond to methanol adsorbed on Cu(I) sites. In addition to these main spectral features, methane activation by Cu-zeolites may give rise to additional ^{13}C NMR signals due to dimethyl ether (DME) adsorbed on zeolite BAS (63–64 ppm)[39, 41] or reduced Cu(I) sites (66–67 ppm).[39] Our recent ^{13}C MAS NMR study demonstrated that methane interaction with Cu-ZSM-5 gives rise to a spectrum (Figure 1) featuring three signals at 52.9, 58.6, and 62.6 ppm which may correspond to different methoxy-like species on the surface of the zeolite. It is clear, that for both MOR and ZSM-5 topologies methane activation

by extra-framework Cu sites results in quite similar ^{13}C MAS NMR spectra for the surface species characterized by three main signals with slightly varying chemical shifts at 50–54, 56–59, and 61–64 ppm. Unfortunately, there is no clear consensus on the assignment of these ^{13}C NMR signals. For instance, the signal at 61–64 ppm was assigned to Cu–O(CH_3)–Cu species,[38] methanol on Cu(I)[39] or dimethyl ether on BAS.[41]

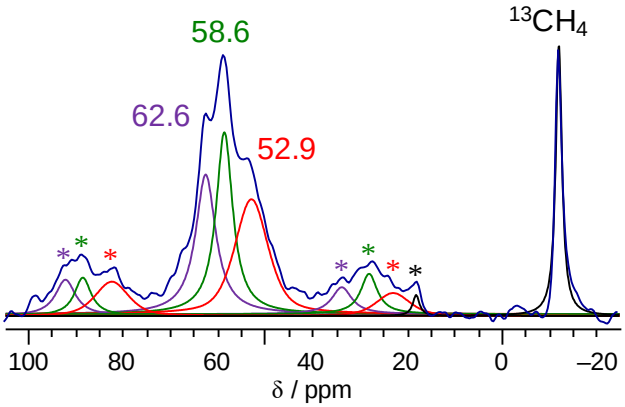

Figure 1. ^{13}C CP/MAS NMR spectrum of surface intermediates formed from methane-^{13}C adsorbed on a Cu-ZSM-5 zeolite. The sample was spun at 3.0 kHz. Asterisks (*) indicate spinning side bands.

To resolve this ambiguity and improve our understanding of the products of methane oxidation by Cu-zeolites, herewith we have performed a combined experimental ^{13}C MAS NMR and computational DFT study. NMR experiments have been carried out to monitor the species formed from methane on Cu/H-ZSM-5 zeolite under different conditions, while DFT calculations of ^{13}C chemical shifts of various methoxy-like species in zeolites, formed at methane activation, have been carried out to support the signals assignment.

2. Experimental Section

Reagents and Materials. Copper(II) acetate monohydrate (≥ 98% purity), benzene (anhydrous, 99.8 % purity), methane-^{13}C (≥99% ^{13}C) and methanol-^{13}C (≥99% ^{13}C) were purchased form Aldrich Chemical Co. Inc. and were used without further purification. Molecular oxygen, industrially produced gas, was used after water removal at liquid nitrogen temperature via freezing and thawing circles.

Zeolite Samples Preparation. The H-form of ZSM-5 zeolite (Si/Al = 17) was provided by Novosibirsk Chemical Concentrates Plant (Novosibirsk, Russia). ICP-OES analysis (Inductively coupled plasma optical emission spectrometry) showed 2.05 wt.% of aluminum in the zeolite sample. The relative amount of extra-framework aluminum species was 4 % as

revealed with ^{27}Al MAS NMR (Figure S1). ^{29}Si MAS NMR spectroscopy (Figure S1) confirmed the Si/Al ratio for the sample to be 17.

The Cu-modified zeolites were prepared with an ion exchange procedure,[42-43] which leads to a partial substitution of zeolite proton sites for hydrated Cu^{2+} cations. Parent H-ZSM-5 zeolite powder was suspended in an aqueous copper(II) acetate solution with pH = 5 and solution/zeolite weight ratio = 10. The suspension was stirred for 48 h at ambient temperature followed by the powder filtration, washing with water, drying at 393 K for 2 h, and calcination in air flow at 773 K for 4 h. Copper(II) acetate solution concentration was 0.0015 and 0.039 M for the preparation of the samples with low and high copper loading, respectively. ICP-OES analysis has shown that the sample with low loading contained 0.10 wt.% of copper (denoted as Cu(0.1)/H-ZSM-5, sample I) and the sample with higher loading contained 1.38 wt.% of copper (denoted as Cu(1.4)/H-ZSM-5, sample II). The determined loadings give Cu/Al atomic ratio of 0.02 and 0.29 for sample I and sample II, respectively. To confirm the proton sites (bridged Si–O(H)–Al groups) substitution by Cu^{2+} cations, the concentration of Si–O(H)–Al groups (Brønsted acid sites, BAS) was measured with ^{1}H MAS NMR method with benzene being used as internal standard according to the procedure described previously.[44-45] The composition of the unit cell of the zeolite samples was estimated based on the ^{1}H MAS NMR quantitative data (Table 1).

NMR Samples Preparation. The NMR monitoring of the intermediates of methane activation were performed by sealing a sample of a zeolite, either sample I or sample II, inside axially highly symmetrical glass ampule of 3.5 mm outer diameter and 10 mm length, capable to fit perfectly into 4 mm zirconia MAS NMR rotor. The zeolite samples of about 25 mg were activated at 673 K under vacuum for 24 h with the residual pressure of less than 10^{-7} bar. Further, molecular oxygen pretreatment was performed by exposing the sample to 500 mbar of dry O_2 followed by heating at 673 K for an hour and evacuation at 423 K for an hour. After the activation procedure, the adsorption of ^{13}C-labeled methane or methanol of 300 $\mu mol/g_{zeolite}$ was performed at the liquid nitrogen temperature, controlled with vacuum gauge (DVR 5, Vacuubrand, Germany). Afterwards, the glass tube with the sample was sealed by flame while keeping the sample under liquid nitrogen to prevent the sample heating.

Solid-State NMR Experiments. MAS NMR spectra were recorded at 9.4 T on a Bruker Avance spectrometer equipped with a broad-band double-resonance 4 mm MAS NMR probe. Zirconia rotors with the inserted sealed glass ampoules were spun at 3-5 kHz by dried compressed air. In order to record ^{27}Al and ^{29}Si MAS NMR spectra, 4 mm rotors were filled

with the powder sample of a zeolite which was preliminary kept under moist atmosphere for several hours. The rotor with the powder inside was spun with the spinning rate of 15.0 and 8.0 kHz for ^{27}Al and ^{29}Si MAS NMR spectra, respectively.

The chemical shift was referenced to tetramethylsilane (TMS) as an external standard for ^{1}H, ^{13}C and ^{29}Si NMR spectra and to 0.1 M $Al(NO_3)_3$ solution for ^{27}Al NMR spectrum with an accuracy of ±0.1 ppm.

Hahn-echo pulse sequence ($\pi/2-\tau-\pi-\tau-$acquisition) was used to record ^{1}H MAS NMR spectra, where τ equals one rotor period (200 μs for 5.0 kHz spinning rate). The excitation pulse length was 5.0 μs ($\pi/2$), and typically 32 scans were accumulated with a 60 s delay. ^{13}C MAS NMR spectra using either only a high-power proton decoupling or in combination with the cross-polarization (CP) technique (^{13}C CP/MAS NMR) were recorded at ambient temperature. The strength of the proton high-power decoupling field B_{RF} was 11.7 G, corresponding to 5.0 μs length of $\pi/2$ ^{1}H pulse and nutation frequency $\nu_{RF} = \gamma/2\pi\ B_{RF}$ = 50 kHz. For the spectra recorded with CP technique, the contact time was 2 ms at the Hartmann−Hahn matching condition of 50 kHz, the delay between scans was 2 s, and the total number of scans was 40000. ^{13}C MAS NMR spectra were recorded with 2000 scans using a 5 s delay. ^{27}Al MAS NMR spectra were obtained with a short 0.6 μs pulse ($\pi/10$), and 10 000 scans were accumulated with a 0.5 s recycle delay. ^{29}Si MAS NMR spectra were recorded with a 5.0 μs pulse ($\pi/2$) and 60 s repetition time, and 1000 scans were acquired for signal accumulation.

Ultraviolet–Visible Near Infrared Diffuse Reflectance Spectroscopy. A Shimadzu UV-2501 PC spectrophotometer equipped with an ISR-240 A diffuse reflectance accessory was used to record the UV–vis DR spectra. The spectral range of 11000–53000 cm^{-1} was monitored with respect to the $BaSO_4$ reflectance standard. The spectra were obtained at ambient temperature. The obtained spectra are presented in the Kubelka–Munk units: F(R) vs wavenumbers. The samples of Cu(0.1)/H-ZSM-5 and Cu(1.4)/H-ZSM-5 were placed inside special quartz cell equipped with UV-grade quartz window. The samples were activated via the same procedure described for NMR samples preparation.

DFT calculations. To model the local coordination environment in ZSM-5 zeolite, a cluster model representing a 10-membered framework ring from the straight channel (10-MR) (Figure 2) was directly cut from the crystal MFI structure obtained from the zeolite database.[46] To introduce anionic negative charge an aluminum atom was placed at the T1 framework position in the cluster. This site has earlier been postulated as the most probable

Al localization site in the MFI structure.[47] To model the structures featuring dicationic species (e.g. containing binuclear Cu sites), a second aluminum atom was placed at the T6 framework position that is separated by two silicon atoms from the T1 site.[21] Dangling bonds on the boundary of the cluster fragments were saturated with hydrogen atoms at 2.5 Å distance from T sites. These clusters were used to model the formation of various methoxy-like intermediates, potentially formed upon methane activation, and simulate their ^{13}C NMR chemical shifts. ChemCraft program was used to visualize molecular structures.[48]

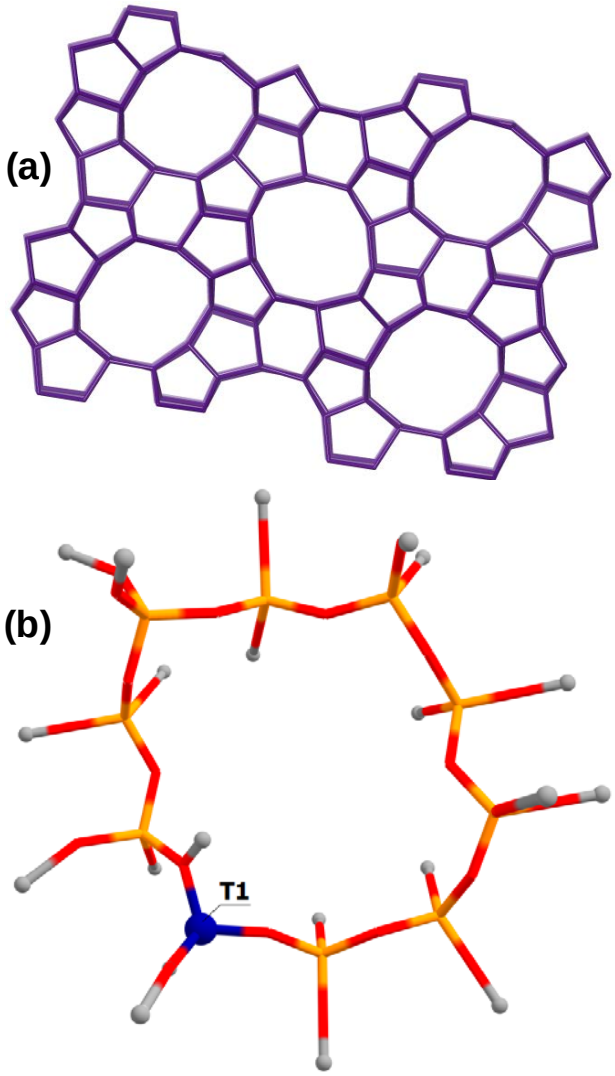

Figure 2. ZSM-5 zeolite framework of MFI type (a).[46] The cluster fragment used to represent ZSM-5 zeolite framework (b).

Spin-unrestricted DFT calculations were carried out using ORCA code[49] with the B3LYP exchange-correlation functional.[50] During the optimization of the geometries of the molecular models, all Si atoms were constrained in their crystallographic positions.[21] Dangled H atoms were also constrained to avoid unrealistic distortions of the model during geometry optimization.[51] 6-31G*[52-53] basis set was used for all (Si, Al, O, H*) atoms of the zeolite

cluster, whereas a larger 6-311+G* [54] basis set was employed for the atoms (Cu, C, H, O) from the extra-framework species.

NMR chemical shielding constants were computed using the GIAO method[55] in combination with the PBE0 functional[56] and aug-cc-pVDZ[57] basis set. Such method, functional and basis set were chosen considering the analysis reported in ref.[58] where reasonably small mean absolute error of 1.71 ^{13}C ppm was demonstrated for this approach. ^{13}C chemical shift was calculated by the following formula:

$$\delta = \sigma_{ref} - \sigma + \delta_{ref.},$$

where σ_{ref} and σ are isotropic chemical shielding of the reference and the examined structures, respectively. Tetramethylsilane was chosen as the reference ($\delta_{ref} = 0$) for which σ_{ref} value was calculated in this study to be 194.9 ppm.

3. Results and Discussion

3.1. Cu/H-ZSM-5 Samples Characterization.

Figure 3 shows UV–vis DR spectra for the samples of Cu-containing zeolites under study, as-prepared and activated under vacuum. As-prepared sample I and sample II exhibit the bands at 12300 cm^{-1} (d-d transition) and related bands at 49000 cm^{-1} (ligand-to-metal charge transfer, LMCT) which are typical of hydrated $[Cu(II)(H_2O)_6]^{2+}$ and $[Cu(II)(OH)(H_2O)_5]^{+}$ cations introduced via the ion exchange and located at cation-exchange sites of the zeolite framework (Si–O$^-$–Al sites).[43, 59-60] An adsorption band at >38000 cm^{-1} is accounted for by the fundamental absorption edge (FAE) of ZSM-5 zeolite (see UV–vis spectrum of parent H-ZSM-5 zeolite in Figure S2). Dehydration of the zeolites under vacuum followed by O_2 treatment at 673 K, leads to the remarkable changes in the spectra: the LMCT band shifts to 44500 cm^{-1} and its intensity increases. The related d-d transition band shifts to 13900 cm^{-1} and undergoes a noticeable broadening. These spectral changes indicate the removal of water ligands and the stabilization of the copper in the state of Cu^{2+} cations at the exchange sites containing two Si–O$^-$–Al units [Z_2Cu(II), where Z = Si–O$^-$–Al].[43, 61-62] Therefore, Z_2Cu(II) sites present in both samples of Cu/H-ZSM-5 zeolite. A minor LMCT band at around 29000 cm^{-1} can also be found in the spectrum of the activated Cu(0.1)/H-ZSM-5 zeolite (Figure 3a). This band can be attributed to another type of monocopper species of Z[Cu(II)(OH)] and/or Z[Cu(II)O] composition[61-63] or to some Cu-oxo clusters such as tricopper $[Cu_3(\mu\text{-}O)_3]^{2+}$,[22] though the latter one is less-likely due to low Cu content in sample I. Hence, our results suggest that the activated sample I contains mostly monocopper Z_2Cu(II) sites, with the

amount of distinct Cu sites being negligible, since other bands, apart from those related to $Z_2Cu(II)$, is hardly detectable in Figure 3a. Contrary, the spectrum of the activated Cu(1.4)/H-ZSM-5 zeolite features a strong band centered at around 32000–33000 cm^{-1} (Figure 3b) which is assigned to $Z_2[Cu_3(\mu\text{-}O)_3]$ species.[22] This points to the presence of additional type of Cu^{2+} sites ($Z_2[Cu_3(\mu\text{-}O)_3]$) in sample II. Previous studies[64] indicated that Cu/H-ZSM-5 materials with Cu/Al of 0.2–0.5 are dominated by $Z_2Cu(II)$ and $Z_2[Cu_3(\mu\text{-}O)_3]$, and this in line with our spectroscopic observation in Figure 3b for sample II having Cu/Al ratio of 0.29 (Table 1).

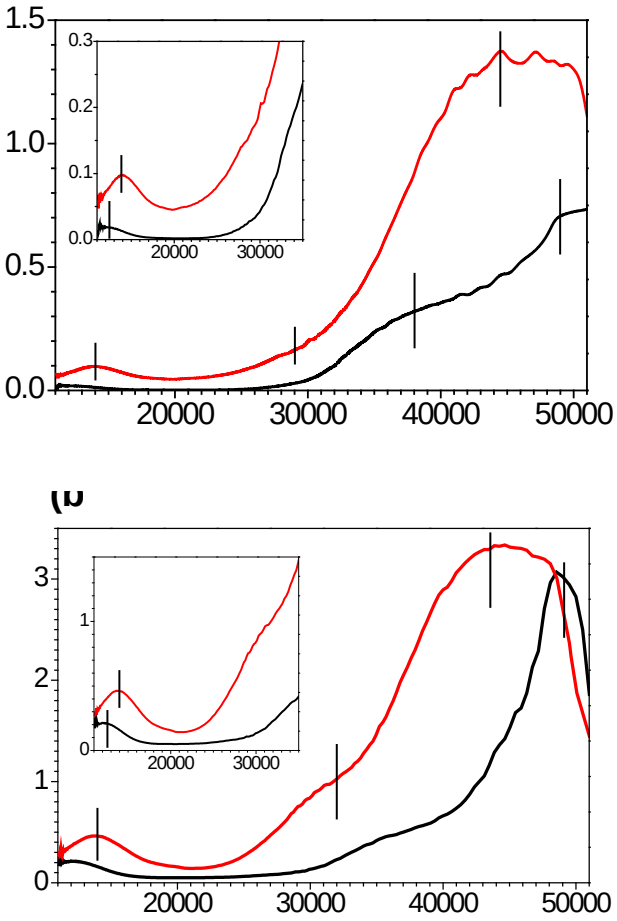

Figure 3. UV–vis DR spectra of Cu(0.1)/H-ZSM-5 (a) and Cu(1.4)/H-ZSM-5 (b) zeolite samples: as-prepared (black lines), after evacuation and treatment with O_2 at 673K (red lines).

Loading of copper into H-ZSM-5 zeolite via the ion exchange leads to the substitution of the protons of the Si–O(H)–Al framework hydroxyl groups for Cu^{2+} hydrated cations, with a theoretical stoichiometry H^+:Cu^{2+} = 2. Further high-temperature activation of Cu-containing zeolite results in the stabilization of Cu^{2+} cations in the pores as $Z_2Cu(II)$ sites,[64] bridged

dicopper $Z_2[Cu_2(\mu\text{-}O)]$ species,[21, 65] and $Z_2[Cu_3(\mu\text{-}O)_3]$ tricopper oxo-clusters[22-23] depending on copper loading and the amount of paired $Si–O^––Al$ sites.[64] It is reasonable to propose that the Cu/Al ratio higher than 0.2[64] can provide neighboring Cu sites which can yield the multinuclear copper species, whereas the low copper content results exclusively in isolated monocopper sites. By comparing the amount residual hydroxyl groups in the activated Cu(0.1)/H-ZSM-5 and Cu(1.4)/H-ZSM-5 samples with Cu/Al ratio, the presence and population of the clustered and isolated monocopper sites can be estimated.

Table 1. Properties of Zeolite Samples.

Sample	ICP-OES data		^{1}H MAS NMR data	Unit cell composition[c]
	Cu / wt.%	Cu/Al atomic ratio[a]	Si–O(H)–Al concentration (BAS) / μmol/g[b]	
H-ZSM-5			940	$H_{5.4}Al_{5.4}Si_{90.6}O_{192}$
Cu(0.1)/H-ZSM-5, sample I	0.10	0.02	900	$Cu^{2+}_{0.11}H_{5.2}Al_{5.4}Si_{90.6}O_{192}$
Cu(1.4)/H-ZSM-5, sample II	1.38	0.29	485	$Cu^{2+}_{1.16}[Cu_3O_3]^{2+}_{0.13}H_{2.8}Al_{5.4}Si_{90.6}O_{192}$

[a]Estimated based on ICP-OES data on Cu and Al content (wt.%).

[b]The accuracy is 5–10 %.

[c]Estimated based on Cu/Al ratio and Si–O(H)–Al groups concentration.

Analysis of Si–O(H)–Al concentration of the zeolite samples was carried out by means of ^{1}H MAS NMR spectroscopy using benzene as internal standard, following the procedure described previously.[44-45] The data on bridged hydroxyls concentration as well as the other properties of the samples are summarized in Table 1. There is good agreement between Cu/Al ratio determined with ICP-OES and the Si–O(H)–Al amount found for Cu(0.1)/H-ZSM-5, if one assumes the presence of only $Z_2Cu(II)$ sites. This strongly favors the conclusion on $Z_2Cu(II)$ being dominant type of copper species in the sample.

In the case of Cu(1.4)/H-ZSM-5, there is remarkable decrease of Si–O(H)–Al concentration. However, the presence of only $Z_2Cu(II)$ at Cu/Al ratio of 0.29 in the sample should result in Si–O(H)–Al amount of 390 μmol/g, which is remarkably lower than the detected one. Obviously, the formation of Cu clusters such as $Z_2[Cu_3(\mu\text{-}O)_3]$, as proposed from the UV–vis DRS data, must also be taken into account. Therefore, the presence of both

$Z_2Cu(II)$ and $Z_2[Cu_3(\mu\text{-}O)_3]$, each substituting the protons of two Si–O(H)–Al sites, as well as Si–O(H)–Al concentration of 485 μmol/g were taken into account to calculate the unit cell composition. In such a case, Cu/Al ratio determined from the unit cell composition perfectly meets the ratio obtained based on ICP-OES data. Thus, we conclude that sample II contains both types of Cu species with the fraction of $Z_2[Cu_3(\mu\text{-}O)_3]$ to be around 10% as follows from ^{1}H MAS NMR quantitative data (Table 1) and assuming that the number of substituted Si–O(H)–Al groups correlates well with Cu/Al ratio for the sample.

3.2. Methane Activation on Cu/H-ZSM-5 Zeolites. ^{13}C MAS NMR Analysis of the Surface Species Formed.

^{13}C MAS NMR spectroscopy was used to study methane interaction with the activated Cu sites in Cu(0.1)/H-ZSM-5 (sample I) and Cu(1.4)/H-ZSM-5 (sample II) zeolites. Figure 4 shows ^{13}C CP/MAS NMR spectra of surface species formed as the result of methane-^{13}C activation on the zeolites after the NMR samples were heated at 523 K for 1 h. The signals observed are located in the region of 53–63 ppm indicating the formation of methoxy-like surface intermediates. Full range ^{13}C CP/MAS NMR and ^{13}C MAS NMR spectra, before and after the heating, are shown in Figures S3 and S4.

The chemical shift of 56–59 ppm is typical for methyl group attached to the framework bridged Si–O^-–Al sites, i.e. the surface methoxide or methoxy species previously detected on various H-form zeolites.[8, 10, 31-32, 66] Therefore, the signal at 58.6 ppm (Figure 4a–c) can be plausibly assigned to surface methoxy Si–O(CH_3)–Al sites, which is in agreement with previously suggested assignments for Cu-ZSM-5 and Cu-MOR,[38-39, 41] but contradicts to another attribution of the signal to Cu–OCH_3 species on Cu-ZSM-5.[40] The signal at 51–53 ppm was previously assigned to strongly adsorbed methanol on the surface of the H-form and Cu-containing zeolites, in particular, on BAS.[38-41, 67] There is a consensus on the origin of such a signal.

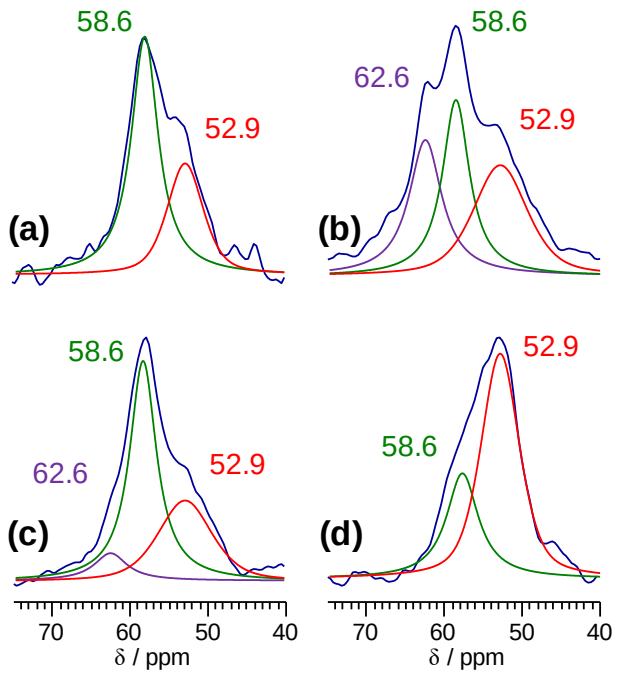

Figure 4. ^{13}C CP/MAS NMR spectra of methane-^{13}C (a–c) and methanol-^{13}C (d) adsorbed on Cu-containing zeolites and heated at 523 K for 1 h. Methane-^{13}C was adsorbed on dehydrated and O_2 treated Cu(0.1)/H-ZSM-5 (a) and Cu(1.4)/H-ZSM-5 (b), on only dehydrated Cu(1.4)/H-ZSM-5 (c). Methanol was adsorbed on dehydrated Cu(1.4)/H-ZSM-5 (d). All spectra were recorded at ambient temperature.

To validate the assignment of the signals at 53–59 ppm, an additional experiment has been performed with methanol-^{13}C adsorbed on Cu(1.4)/H-ZSM-5 zeolite (Figure 4d). Two signals at 52.9 and 58.6 ppm could be clearly distinguished in the resulting ^{13}C MAS NMR spectrum similar to the spectral features observed upon methane activation (Figures 4a–c). The major signal at 52.9 can be directly related to methanol adsorbed on BAS. The minor signal at 58.6 ppm evidences the formation of surface-bound methoxide resulting from the transformation of metahanol over the residual BAS of the zeolite.[68-69]

Importantly, methanol-^{13}C was adsorbed on Cu(1.4)/H-ZSM-5 zeolite which was not treated with O_2 at high temperature and therefore contained Cu(I) sites resulting from partial Cu(II) sites reduction.[43, 59, 62, 70] However, no specific signals either at >62 ppm previously attributed to methanol adsorbed on Cu(I)[39] could be observed in Figure 4d. This implies that the complex of methanol with Cu(I) sites as intermediate does not form at methane activation on Cu(1.4)/H-ZSM-5 zeolite.

The third detected signal in Figure 4b with the chemical shift of 62.6 ppm still requires an assignment. A similar signal at 61.2 ppm was first observed by Narsimhan et al.[38] for methane activation on Cu-MOR catalyst and it was attributed to methyl group attached to Cu–

O(CH_3)–Cu bridging species. A similar signal at 62 ppm was assigned by Sushkevich et al.[39] to methanol adsorbed on Cu(I) sites. Dyballa et al.[41] suggested that the signal at 63–64 ppm arose from dimethyl ether adsorbed on BAS. However, a pathway to dimethyl either formation has not been discussed. Validation of these suggested assignments can be made by comparing the behavior of sample I and sample II, since only the latter one contains Cu–O–Cu fragments due to clustered Cu sites. The results in Figure 4a–c show that the signal at 62.6 ppm is exclusively formed over the Cu-rich sample II featuring such bridging Cu–O–Cu moieties (Figure 4b), while it is not detected for sample I containing only monocopper species (Figure 4a). These results indicate a direct correlation between the presence Cu–O–Cu moieties in the zeolite and the signal at 61–63 ppm, which most likely should be attributed to Cu–O(CH_3)–Cu type species. The exact structure and the composition of the intermediate, either methanol strongly adsorbed in between two Cu atoms[23] (Cu–($HOCH_3$)–Cu species) or methoxide[38] (Cu–O(CH_3)–Cu species), can be clarified with the aid of corresponding DFT calculations (*vide infra*).

3.3. DFT Calculations of ^{13}C Chemical Shifts of Possible Methane Activation Intermediates.

^{13}C CP/MAS NMR data reported above provide an insight into the nature of the methoxy-like intermediates formed upon methane activation by Cu-containing zeolites. To further rationalize the NMR data and gain a better molecular-level understanding of the intermediates, we have performed DFT calculations for the number of model structures representing the possible methoxy species in Cu-ZSM-5 zeolite. Figures 5 and 6 summarize the optimized structures of the computed intermediates and adsorption complexes. The computed NMR parameters that is the respective ^{13}C chemical shifts are summarized in Table 2 (see column "Calculated"). Table 2 also shows our assignments of the ^{13}C chemical shifts based on NMR experiments performed (see column "Experimental") as well as the assignments suggested in literature. Therefore, theoretical and experimental data reported in this work can be compared with those found in other studies.

To validate the chosen method for calculations of ^{13}C chemical shifts, we first computed the chemical shift of a lattice-bound methoxy group. The optimized structure of the model representing such a Si–O(CH_3)–Al moiety is shown in Figure 5a. The computed ^{13}C chemical shift for Si–O(CH_3)–Al structure is 58.2 ppm, which is in an excellent agreement with the

experimental value of 58.6 ppm found in this work for Cu-ZSM-5 and 59 ppm for the surface methoxy species detected on different ZSM-5 materials.[8, 10, 31, 66]

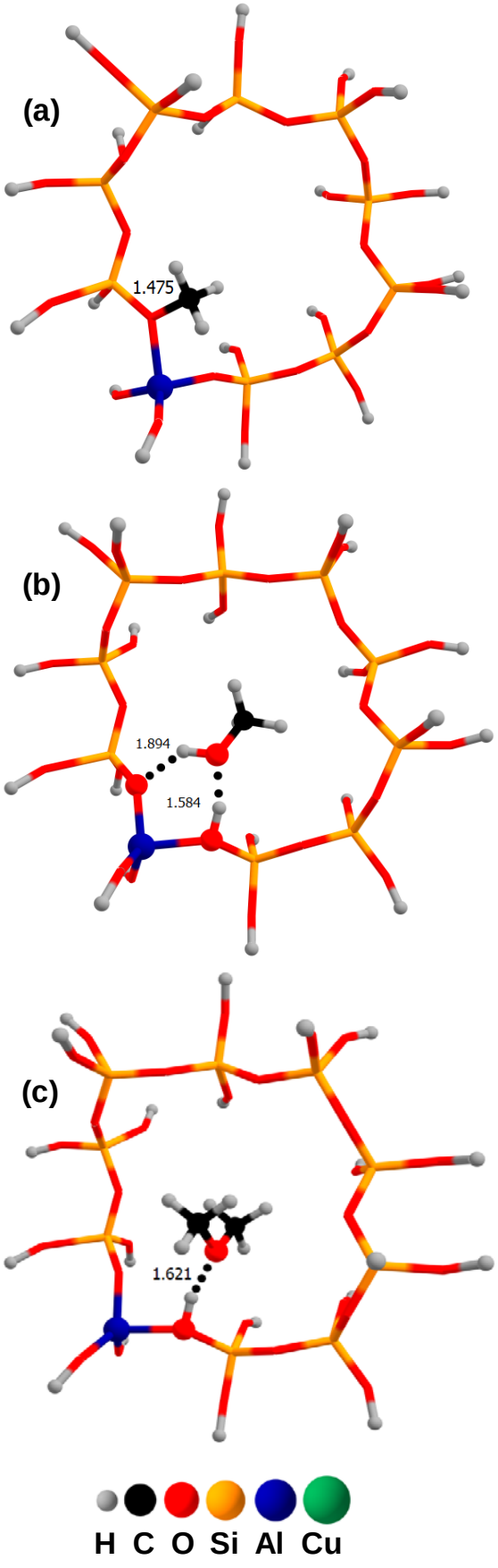

5

Figure 5. Optimized structures, which were used to calculate the ^{13}C NMR chemical shifts of Si–O(CH_3)–Al (a), CH_3OH adsorbed on BAS (b), DME adsorbed on BAS (c). Optimized distances are shown in Å units.

The calculations predict the chemical shift of 52.5 ppm for the adsorption complexes of CH_3OH with BAS (Figure 5b), whereas the adsorption complex with a Cu(I) cation (Figure 6a) would give rise to the signal with a chemical shift of 64.8 ppm. Experimentally observed signal at 52.9 ppm (Figure 4) corresponds to the former adsorption complex, whereas the latter one is not observed experimentally in this study. So, there is good agreement between DFT and NMR results in this work. Our calculations support the earlier assignment of the signal at 52.9 ppm to methanol adsorbed on zeolite BAS of Cu-ZSM-5 and Cu-MOR.[38-40]

Table 2. DFT predicted and experimentally observed chemical shifts assigned to various methoxy-like species.

Species	^{13}C NMR chemical shift / ppm			Reference for literature data
	Calculated	Experimental	Literature data	
Si–O(CH_3)–Al	58.2	58.6	56–59	8, 10, 31-32, 38-39, 41, 66
CH_3OH on Cu(I)	64.8	N/D[a]	62	39
$(CH_3)_2O$ on Cu(I)	66.9 and 67.6	N/D[a]	67	39
CH_3OH on BAS	52.5	52.9	51–53	38-41, 67
$(CH_3)_2O$ on BAS	58.6 and 59.4	N/D[a]	59–60; 62–63 (end-on; side-on)	31, 39, 41, 67
Cu–O(CH_3)–Cu	59.2	[b]	61.2	38
Cu–($HOCH_3$)–Cu	62.8	62.6	[c]	[c]

[a]N/D means that the signal was not detected.

[b]Species are not formed under conditions studied.

[c]There was no signal reported for such assignment.

Calculation of ^{13}C chemical shift for the adsorption complex of the dimethyl ether (DME) (end-on type of adsorption) on BAS (Figure 5c) predicts values of 58.6 and 59.4 ppm, respectively, which is in good agreement with the experimental value of 59–60 ppm reported in previous studies on H-ZSM-5.[31, 67] Our calculations give slightly different values for the chemical shift of two carbon atoms of DME adsorbed on BAS (Figure 5c) and on a Cu(I) site (Figure 6b). This can be explained by an asymmetry of the optimized structures of the

adsorption complexes which results in different local geometry and, therefore, different shielding constants and chemical shifts of the carbon atoms.

Adsorption complex of DME (Figure 6b) with Cu(I) site was also considered. The calculated values of ^{13}C chemical shift for this species are 66.9 and 67.6 ppm, which are in good agreement with the chemical shift of 67 ppm observed earlier for such type of a complex.[39] The absence of the signal at 67 ppm in Figure 4 implies that the complex of DME with Cu(I) site is not formed in our case. Moreover, DME formation from methane under water free conditions on Cu-ZSM-5 or Cu-MOR has never been observed. DME was detected to be formed during steam purging of Cu-MOR,[22] probably as the product of methanol dehydration. Taking such reasoning into account, it is plausible to suggest that the observation of dimethyl ether on Cu-containing zeolites reported earlier[39, 41] can be related with the presence of some quantity of water in the zeolite samples, which was not the case in the current work. Thus, our DFT calculations and NMR data allow us to conclude that DME should be excluded from the list of possible intermediates of methane activation on Cu-modified zeolites under conditions of our experiments.

Two more possible structures represent the methoxy-like intermediates that may contribute to the signal at 62.6 ppm in Figure 4. It is worth mentioning that this signal should belong to the intermediate formed on Cu–O–Cu sites according to NMR results discussed above. The first structure is Cu–O(CH_3)–Cu (Figure 6c), i.e., the methyl group bound to extra-framework oxygen of Cu–O–Cu fragment. Such assignment was proposed in ref.[38] for Cu-MOR zeolite, and Cu–O(CH_3)–Cu species were theoretically predicted to be stable intermediates.[28] The second structure is Cu–($HOCH_3$)–Cu intermediate (methanol adsorption complex with two Cu(I) sites) (Figure 6d) suggested as the alternative stable intermediate of methane activation.[23] DFT calculations show Cu–O(CH_3)–Cu structure (Figure 6c) gives the signal with the ^{13}C chemical shift of 59.2 ppm, which in significantly different from the experimentally observed signal at 62.6 ppm (Figure 4b). On the other hand, the calculation of the shift for Cu–($HOCH_3$)–Cu structure provides a reasonable value of 62.8 ppm which is in line with proposed assignment of the experimentally detected signal to the methoxy-like species bound to two Cu atoms.

Thus, the results allow us to distinguish between to theoretically predicted stable intermediates of methane activation on Cu–O–Cu sites of $[Cu_2(\mu\text{-}O)]^{2+}$ or $[Cu_3(\mu\text{-}O)_3]^{2+}$ species. In our particular case, $[Cu_2(\mu\text{-}O)]^{2+}$ structure was selected and examined here for the calculations. NMR and DFT data of the current study allow us to infer that Cu–($HOCH_3$)–

Cu species is a stable intermediate of methane activation on Cu-containing ZSM-5 zeolites with Cu–O–Cu active fragments.

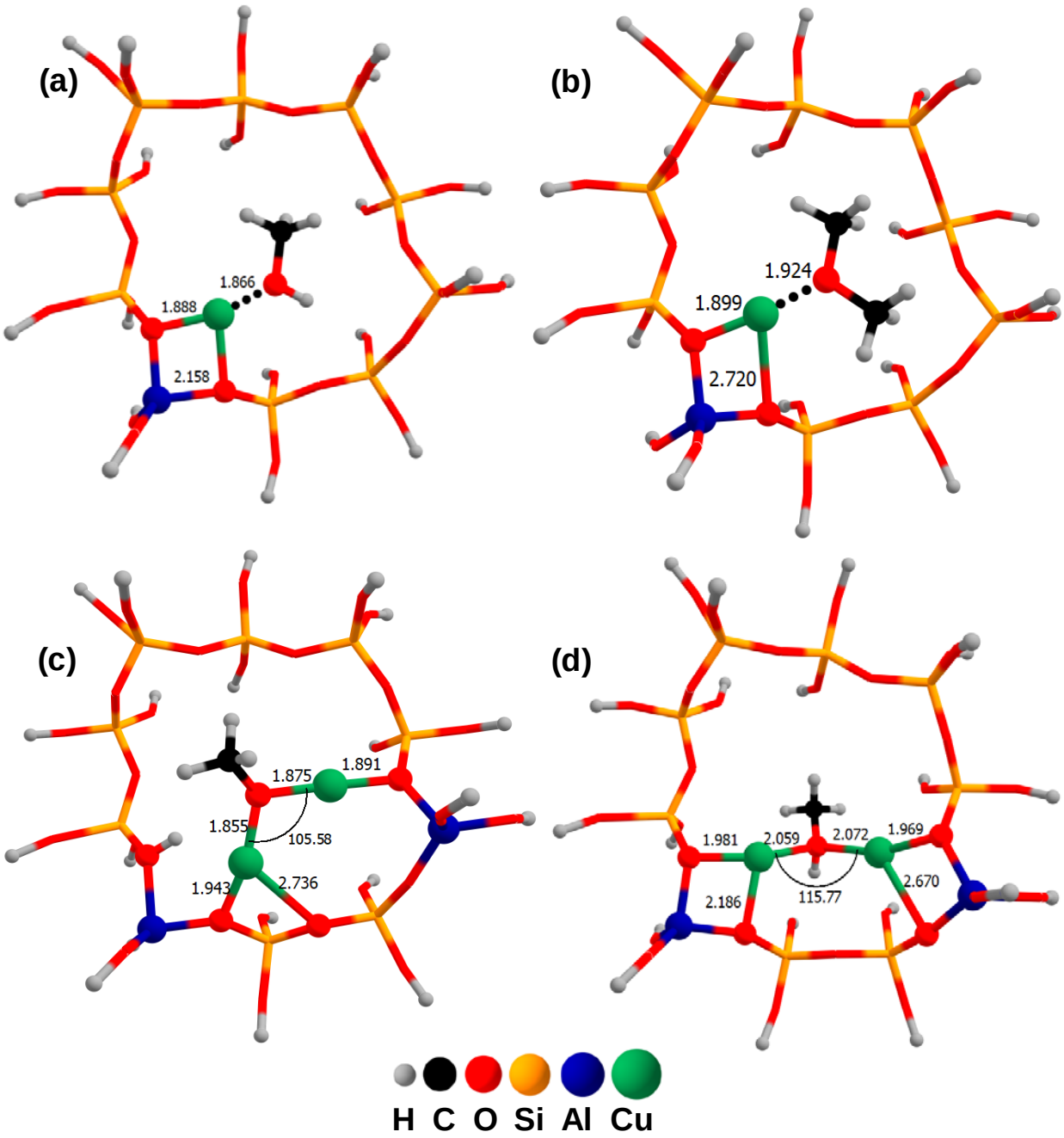

Figure 6. Optimized structures of CH_3OH adsorbed on Cu(I) site (a), DME adsorbed on Cu(I) site (b), Cu–O(CH_3)–Cu (c), Cu–($HOCH_3$)–Cu (d).

3.4. Mechanisms of Methane Activation on Cu/H-ZSM-5 Zeolites.

The combined NMR and DFT study on the nature of surface intermediates of methane-to-methanol transformation on Cu/H-ZSM-5 zeolites has provided new insights onto the mechanisms of methane activation and conversion assisted with different Cu sites. The

structure and composition of the identified intermediates are in favor of particular methane activation mechanisms recently suggested based on theoretical and experimental studies. The formation of only three types of methoxy-like intermediates on Cu/H-ZSM-5 is confirmed. As evidenced with ^{13}C MAS NMR and supported with model DFT calculations, methane transforms over Cu/H-ZSM-5 to surface methoxide Si–O(CH_3)–Al (58.6 ppm), methanol adsorption complex with BAS (52.9 ppm), and methanol adsorption complex with two Cu atoms Cu–($HOCH_3$)–Cu (62.6 ppm). Importantly, the former intermediate is detected only when $Z_2[Cu_3(\mu\text{-}O)_3]$ sites are generated in the zeolite after the treatment with O_2. The other two intermediates are formed even when only $Z_2Cu(II)$ sites are present in the zeolite material.

Thus, methane C–H bond homolytic cleavage mechanism involving methyl radical rebound step, described previously as one of the options,[23, 28, 71] seems to be realized for $Z_2[Cu_3(\mu\text{-}O)_3]$ sites in Cu/H-ZSM-5 since this pathway of methane transformation is predicted to yield stable intermediate of Cu–($HOCH_3$)–Cu composition. Based on the data reported in this work, other alternative mechanisms for $Z_2[Cu_3(\mu\text{-}O)_3]$ sites involving Cu–O(CH_3)–Cu species formation can be considered as unrealizable under the conditions studied here. The same rebound mechanism can be also proposed for methane activation on various alternative di- and tricopper oxo-clusters since same Cu–($HOCH_3$)–Cu intermediate was observed with ^{13}C MAS NMR for different Cu-MOR and Cu-ZSM-5 zeolites containing Cu–O–Cu extra-framework species.[38-41] The formation of other two intermediates, Si–O(CH_3)–Al and methanol on BAS, were detected for Cu/H-ZSM-5 dominated by monocopper $Z_2Cu(II)$ sites. This strongly supports the suggestion on the involvement of monocopper Cu(II) species in methane C–H bond activation via either homolytic or heterolytic pathways. Note, the role of other monocopper sites (Z[Cu(II)(OH)] or Z[Cu(II)O], observed as minor species in Cu(0.1)/H-ZSM-5) can be also important as predicted with DFT methods.[24] Possible participation of monocopper sites of Cu-ZSM-5 zeolite in methane activation process has been recently studied experimentally.[72] The proposed mechanism including heterolytic C–H bond cleavage, however, requires further investigation.

4. Conclusions

Two samples of zeolite H-ZSM-5 containing 0.1 wt.% Cu (Cu(0.1)/H-ZSM-5, sample I) and 1.4 wt.% Cu (Cu(1.4)/H-ZSM-5, sample II) have been prepared. Both qualitative UV–vis DRS and quantitative ^1H MAS NMR analysis of the state of copper in the zeolites have shown that the sample I contains Cu in the form of $Z_2Cu(II)$ species (Z = Si–O^-–Al site),

while for the sample II both $Z_2Cu(II)$ and $Z_2[Cu_3(\mu\text{-}O)_3]$ species are present in the zeolite. Activation of methane on these samples results in the formation of three different surface methoxy-like intermediates with the signals at 52.9, 58.6, and 62.6 ppm in ^{13}C CP/MAS NMR spectrum. All three signals are detected for the sample II, containing Cu–O–Cu extra-framework sites in the form of tricopper $[Cu_3(\mu\text{-}O)_3]^{2+}$ oxo-clusters, whereas only two signals at 52.9 and 58.6 ppm are observed for the sample I, where the Cu–O–Cu sites are absent. ^{13}C MAS NMR experiments with methane-^{13}C and methanol-^{13}C adsorbed on the samples I and II allowed us to assign the signal at 62.6 ppm to methanol adsorbed in between two copper atoms (Cu–($HOCH_3$)–Cu species). The signal at 58.6 ppm is attributed to methyl group attached to framework bridged Si–O^-–Al site (Si–O(CH_3)–Al species), and the signal at 52.9 ppm can be assigned to methanol adsorbed on the Brønsted acid site of the zeolite. Such assignment has been fully confirmed by DFT calculations of ^{13}C chemical shifts for a number of methoxy-like species which may be formed on the surface of Cu-containing zeolites with BAS and copper oxo-clusters. The identification of the intermediates formed in the course of methane to methanol transformation allows further evaluation on the mechanism of methane activation on different Cu sites present in the zeolites. In particular, the mechanism with methyl radical rebound step[23, 28, 71] seems to be the one which is realized for ZSM-5 zeolite containing $Z_2[Cu_3(\mu\text{-}O)_3]$ oxo-clusters, because of the observation of methanol strongly adsorbed in between two Cu atoms, i.e., Cu–($HOCH_3$)–Cu species. The formation of other two intermediates, Si–O(CH_3)–Al and CH_3OH adsorbed on BAS, may be indicative of the involvement of $Z_2Cu(II)$ or other monocopper sites into methane activation.[72]

AUTHOR INFORMATION

Corresponding Authors

E-mail: stepanov@catalysis.ru (A.G. Stepanov)

E-mail: E.A.Pidko@tudelft.nl (E.A. Pidko)

Author Contributions

The manuscript was written through contributions of all authors. All authors have given approval to the final version of the manuscript.

Notes

The authors declare no competing financial interest.

SUPPORTING INFORMATION

^{27}Al and ^{29}Si MAS NMR spectra of H-ZSM-5, UV−vis DR spectra of H-ZSM-5 and Cu/H-ZSM-5 at ambient conditions, ^{13}C MAS and CP/MAS NMR spectra of methane-^{13}C and methanol-^{13}C on Cu/H-ZSM-5 zeolites.

ACKNOWLEDGMENT

This work was financially supported by the Russian Science Foundation (Grant No. 18-73-00016) and, in part (NMR facilities maintenance), by the Ministry of Science and Higher Education of the Russian Federation (Project No. AAAA-A17-117041710084-2).

REFERENCES

1. McFarland, E. Unconventional Chemistry for Unconventional Natural Gas. *Science* **2012**, *338*, 340–342.

2. Gabrienko, A. A.; Arzumanov, S. S.; Toktarev, A. V.; Danilova, I. G.; Prosvirin, I. P.; Kriventsov, V. V.; Zaikovskii, V. I.; Freude, D.; Stepanov, A. G. Different Efficiency of Zn^{2+} and ZnO Species for Methane Activation on Zn-Modified Zeolite. *ACS Catal.* **2017**, *7*, 1818–1830.

3. Baba, T.; Abe, Y.; Nomoto, K.; Inazu, K.; Echizen, T.; Ishikawa, A.; Murai, K. Catalytic Transformation of Methane over In-Loaded ZSM-5 Zeolite in the Presence of Ethene. *J. Phys. Chem. B* **2005**, *109*, 4263–4268.

4. Chen, G.; Zhao, Y.; Shang, L.; Waterhouse, G. I. N.; Kang, X.; Wu, L.-Z.; Tung, C.-H.; Zhang, T. Recent Advances in the Synthesis, Characterization and Application of Zn^{+}-Containing Heterogeneous Catalysts. *Adv. Sci.* **2016**, *3*, 1500424.

5. Gabrienko, A. A.; Arzumanov, S. S.; Luzgin, M. V.; Stepanov, A. G.; Parmon, V. N. Methane Activation on Zn^{2+}-Exchanged ZSM-5 Zeolites. The Effect of Molecular Oxygen Addition. *J. Phys. Chem. C* **2015**, *119*, 24910–24918.

6. Choudhary, V. R.; Mondal, K. C.; Mulla, S. A. R. Simultaneous Conversion of Methane and Methanol into Gasoline over Bifunctional Ga-, Zn-, In-, and/or Mo-Modified ZSM-5 Zeolites. *Angew. Chem. Int. Ed.* **2005**, *44*, 4381–4385.

7. Gabrienko, A. A.; Arzumanov, S. S.; Toktarev, A. V.; Freude, D.; Haase, J.; Stepanov, A. G. Hydrogen H/D Exchange and Activation of C_1 - n-C_4 Alkanes on Ga-Modified Zeolite

BEA Studied with ^{1}H Magic Angle Spinning Nuclear Magnetic Resonance in Situ. *J. Phys. Chem. C* **2011**, *115*, 13877–13886.

8. Gabrienko, A. A.; Arzumanov, S. S.; Moroz, I. B.; Prosvirin, I. P.; Toktarev, A. V.; Wang, W.; Stepanov, A. G. Methane Activation on In-Modified ZSM-5: The State of Indium in the Zeolite and Pathways of Methane Transformation to Surface Species. *J. Phys. Chem. C* **2014**, *118*, 8034–8043.

9. Baba, T. Conversion of Methane over Ag^{+}-Exchanged Zeolite in the Presence of Ethene. *Catal. Surv. Asia* **2005**, *9*, 147–154.

10. Gabrienko, A. A.; Arzumanov, S. S.; Moroz, I. B.; Toktarev, A. V.; Wang, W.; Stepanov, A. G. Methane Activation and Transformation on Ag/H-ZSM-5 Zeolite Studied with Solid-State NMR. *J. Phys. Chem. C* **2013**, *117*, 7690–7702.

11. Ravi, M.; Ranocchiari, M.; van Bokhoven, J. A. The Direct Catalytic Oxidation of Methane to Methanol—A Critical Assessment. *Angew. Chem. Int. Ed.* **2017**, *56*, 16464–16483.

12. Vanelderen, P.; Hadt, R. G.; Smeets, P. J.; Solomon, E. I.; Schoonheydt, R. A.; Sels, B. F. Cu-ZSM-5: A Biomimetic Inorganic Model for Methane Oxidation. *J. Catal.* **2011**, *284*, 157–164.

13. Ruscic, B. Active Thermochemical Tables: Sequential Bond Dissociation Enthalpies of Methane, Ethane, and Methanol and the Related Thermochemistry. *J. Phys. Chem. A* **2015**, *119*, 7810–7837.

14. Rostrup-Nielsen, J. R.; Sehested, J.; Norskov, J. K. In *Adv. Catal.*; Gates, B. C., Knozinger, H., Eds.; Elsevier Academic Press Inc: San Diego, 2002; Vol. 47, pp 65–139.

15. Olivos-Suarez, A. I.; Szecsenyi, A.; Hensen, E. J. M.; Ruiz-Martinez, J.; Pidko, E. A.; Gascon, J. Strategies for the Direct Catalytic Valorization of Methane Using Heterogeneous Catalysis: Challenges and Opportunities. *ACS Catal.* **2016**, *6*, 2965–2981.

16. Ravi, M.; Sushkevich, V. L.; Knorpp, A. J.; Newton, M. A.; Palagin, D.; Pinar, A. B.; Ranocchiari, M.; van Bokhoven, J. A. Misconceptions and Challenges in Methane-to-Methanol over Transition-Metal-Exchanged Zeolites. *Nat. Catal.* **2019**, *2*, 485–494.

17. Wang, B.; Albarracín-Suazo, S.; Pagán-Torres, Y.; Nikolla, E. Advances in Methane Conversion Processes. *Catal. Today* **2017**, *285*, 147–158.

18. Hakemian, A. S.; Rosenzweig, A. C. The Biochemistry of Methane Oxidation. *Annu. Rev. Biochem.* **2007**, *76*, 223–241.

19. Hanson, R. S.; Hanson, T. E. Methanotrophic Bacteria. *Microbiol. Rev.* **1996**, *60*, 439–471.

20. Groothaert, M. H.; Smeets, P. J.; Sels, B. F.; Jacobs, P. A.; Schoonheydt, R. A. Selective Oxidation of Methane by the Bis(mu-oxo)dicopper Core Stabilized on ZSM-5 and Mordenite Zeolites. *J. Am. Chem. Soc.* **2005**, *127*, 1394–1395.

21. Woertink, J. S.; Smeets, P. J.; Groothaert, M. H.; Vance, M. A.; Sels, B. F.; Schoonheydt, R. A.; Solomon, E. I. A [Cu(2)O](2+) Core in Cu-ZSM-5, the Active Site in the Oxidation of Methane to Methanol. *P. Natl. Acad. Sci. USA* **2009**, *106*, 18908–18913.

22. Grundner, S.; Markovits, M. A. C.; Li, G.; Tromp, M.; Pidko, E. A.; Hensen, E. J. M.; Jentys, A.; Sanchez-Sanchez, M.; Lercher, J. A. Single-Site Trinuclear Copper Oxygen Clusters in Mordenite for Selective Conversion of Methane to Methanol. *Nat. Commun.* **2015**, *6*, 7546.

23. Li, G.; Vassilev, P.; Sanchez-Sanchez, M.; Lercher, J. A.; Hensen, E. J. M.; Pidko, E. A. Stability and Reactivity of Copper Oxo-Clusters in ZSM-5 Zeolite for Selective Methane Oxidation to Methanol. *J. Catal.* **2016**, *338*, 305–312.

24. Kulkarni, A. R.; Zhao, Z.-J.; Siahrostami, S.; Nørskov, J. K.; Studt, F. Monocopper Active Site for Partial Methane Oxidation in Cu-Exchanged 8MR Zeolites. *ACS Catal.* **2016**, *6*, 6531–6536.

25. Mahyuddin, M. H.; Tanaka, T.; Staykov, A.; Shiota, Y.; Yoshizawa, K. Dioxygen Activation on Cu-MOR Zeolite: Theoretical Insights into the Formation of Cu_2O and Cu_3O_3 Active Species. *Inorg. Chem.* **2018**, *57*, 10146–10152.

26. Mahyuddin, M. H.; Staykov, A.; Shiota, Y.; Miyanishi, M.; Yoshizawa, K. Roles of Zeolite Confinement and Cu–O–Cu Angle on the Direct Conversion of Methane to Methanol by $[Cu_2(\mu\text{-}O)]^{2+}$-Exchanged AEI, CHA, AFX, and MFI Zeolites. *ACS Catal.* **2017**, *7*, 3741–3751.

27. Yumura, T.; Hirose, Y.; Wakasugi, T.; Kuroda, Y.; Kobayashi, H. Roles of Water Molecules in Modulating the Reactivity of Dioxygen-Bound Cu-ZSM-5 toward Methane: A Theoretical Prediction. *ACS Catal.* **2016**, *6*, 2487–2495.

28. Sushkevich, V. L.; Palagin, D.; Ranocchiari, M.; van Bokhoven, J. A. Selective Anaerobic Oxidation of Methane Enables Direct Synthesis of Methanol. *Science* **2017**, *356*, 523–527.

29. Arzumanov, S. S.; Gabrienko, A. A.; Freude, D.; Stepanov, A. G. Competitive Pathways of Methane Activation on Zn^{2+}-Modified ZSM-5 Zeolite: H/D Hydrogen Exchange with Brønsted Acid Sites versus Dissociative Adsorption to Form Zn-Methyl Species. *Catal. Sci. Technol.* **2016**, *6*, 6381–6388.

30. Luzgin, M. V.; Gabrienko, A. A.; Rogov, V. A.; Toktarev, A. V.; Parmon, V. N.; Stepanov, A. G. The "Alkyl" and "Carbenium" Pathways of Methane Activation on Ga-

Modified Zeolite BEA: ^{13}C Solid-State NMR and GC-MS Study of Methane Aromatization in the Presence of Higher Alkane. *J. Phys. Chem. C* **2010**, *114*, 21555–21561.

31. Wang, W.; Seiler, M.; Hunger, M. Role of Surface Methoxy Species in the Conversion of Methanol to Dimethyl Ether on Acidic Zeolites Investigated by in Situ Stopped-Flow MAS NMR Spectroscopy. *J. Phys. Chem. B* **2001**, *105*, 12553–12558.

32. Jiang, Y.; Hunger, M.; Wang, W. On the Reactivity of Surface Methoxy Species in Acidic Zeolites. *J. Am. Chem. Soc.* **2006**, *128*, 11679–11692.

33. Ivanova, I. I.; Kolyagin, Y. G. Impact of In Situ MAS NMR Techniques to the Understanding of the Mechanisms of Zeolite Catalyzed Reactions. *Chem. Soc. Rev.* **2010**, *39*, 5018–5050.

34. Kolyagin, Y. G.; Ivanova, I. I.; Ordomsky, V. V.; Gedeon, A.; Pirogov, Y. A. Methane Activation over Zn-Modified MFI Zeolite: NMR Evidence for Zn-Methyl Surface Species Formation. *J. Phys. Chem. C* **2008**, *112*, 20065–20069.

35. Wang, X. M.; Xu, J.; Qi, G. D.; Wang, C.; Wang, W. Y.; Gao, P.; Wang, Q.; Liu, X. L.; Feng, N. D.; Deng, F. Carbonylation of Ethane with Carbon Monoxide over Zn-Modified ZSM-5 Zeolites Studied by in Situ Solid-State NMR Spectroscopy. *J. Catal.* **2017**, *345*, 228–235.

36. Xu, J.; Zheng, A. M.; Wang, X. M.; Qi, G. D.; Su, J. H.; Du, J. F.; Gan, Z. H.; Wu, J. F.; Wang, W.; Deng, F. Room Temperature Activation of Methane over Zn Modified H-ZSM-5 Zeolites: Insight from Solid-State NMR and Theoretical Calculations. *Chem. Sci.* **2012**, *3*, 2932–2940.

37. Wang, X. M.; Qi, G. D.; Xu, J.; Li, B. J.; Wang, C.; Deng, F. NMR-Spectroscopic Evidence of Intermediate-Dependent Pathways for Acetic Acid Formation from Methane and Carbon Monoxide over a ZnZSM-5 Zeolite Catalyst. *Angew. Chem. Int. Ed.* **2012**, *51*, 3850–3853.

38. Narsimhan, K.; Michaelis, V. K.; Mathies, G.; Gunther, W. R.; Griffin, R. G.; Román-Leshkov, Y. Methane to Acetic Acid over Cu-Exchanged Zeolites: Mechanistic Insights from a Site-Specific Carbonylation Reaction. *J. Am. Chem. Soc.* **2015**, *137*, 1825–1832.

39. Sushkevich, V. L.; Verel, R.; Bokhoven, J. A. v. Pathways of Methane Transformation over Copper-Exchanged Mordenite as Revealed by in situ NMR and IR Spectroscopy. *Angew. Chem. Int. Ed.* **2019**, *58*, 2–11.

40. Wu, J.-F.; Gao, X.-D.; Wu, L.-M.; Wang, W. D.; Yu, S.-M.; Bai, S. Mechanistic Insights on the Direct Conversion of Methane into Methanol over Cu/Na–ZSM-5 Zeolite: Evidence from EPR and Solid-State NMR. *ACS Catal.* **2019**, *9*, 8677–8681.

41. Dyballa, M.; Thorshaug, K.; Pappas, D. K.; Borfecchia, E.; Kvande, K.; Bordiga, S.; Berlier, G.; Lazzarini, A.; Olsbye, U.; Beato, P.; Svelle, S.; Arstad, B. Zeolite Surface Methoxy Groups as Key Intermediates in the Stepwise Conversion of Methane to Methanol. **2019**, *11*, 5022–5026.

42. Yashnik, S. A.; Salnikov, A. V.; Vasenin, N. T.; Anufrienko, V. F.; Ismagilov, Z. R. Regulation of the Copper-Oxide Cluster Structure and DeNOx Activity of Cu-ZSM-5 Catalysts by Variation of OH/Cu^{2+}. *Catal. Today* **2012**, *197*, 214–227.

43. Yashnik, S. A.; Ismagilov, Z. R.; Anufrienko, V. F. Catalytic Properties and Electronic Structure of Copper Ions in Cu-ZSM-5. *Catal. Today* **2005**, *110*, 310–322.

44. Stepanov, A. G. In *Zeolites and Zeolite-like Materials*; Sels, B. F., Kustov, L. M., Eds.; Elsevier Inc.: 2016; pp 137–188.

45. Gabrienko, A. A.; Danilova, I. G.; Arzumanov, S. S.; Pirutko, L. V.; Freude, D.; Stepanov, A. G. Direct Measurement of Zeolite Brønsted Acidity by FTIR Spectroscopy: Solid-State ^{1}H MAS NMR Approach for Reliable Determination of the Integrated Molar Absorption Coefficients. *J. Phys. Chem. C* **2018**, *122*, 25386–25395.

46. Baerlocher, C.; McCusker, L. B. Database of Zeolite Structures. http://www.iza-structure.org/databases/ (accessed Dec 10, 2018).

47. Dib, E.; Mineva, T.; Veron, E.; Sarou-Kanian, V.; Fayon, F.; Alonso, B. ZSM-5 Zeolite: Complete Al Bond Connectivity and Implications on Structure Formation from Solid-State NMR and Quantum Chemistry Calculations. *J. Phys. Chem. Lett.* **2018**, *9*, 19–24.

48. Yang, X. Structural Identification of Intermediate Aluminum Species in Usy Zeolites Using High-Resolution and Spin-Lattice Relaxation Al-27 NMR. *J. Phys. Chem.* **1995**, *99*, 1276–1280.

49. Neese, F. The ORCA Program System. *WIREs Comput. Mol. Sci.* **2012**, *2*, 73–78.

50. Becke, A. D. Density-Functional Thermochemistry. III. The Role of Exact Exchange. *J. Chem. Phys.* **1993**, *98*, 5648–5652.

51. Van der Mynsbrugge, J.; Visur, M.; Olsbye, U.; Beato, P.; Bjørgen, M.; Van Speybroeck, V.; Svelle, S. Methylation of Benzene by Methanol: Single-Site Kinetics over H-ZSM-5 and H-Beta Zeolite Catalysts. *J. Catal.* **2012**, *292*, 201–212.

52. Hehre, W. J.; Ditchfield, R.; Pople, J. A. Self—Consistent Molecular Orbital Methods. XII. Further Extensions of Gaussian—Type Basis Sets for Use in Molecular Orbital Studies of Organic Molecules. *J. Chem. Phys.* **1972**, *56*, 2257–2261.

53. Francl, M. M.; Pietro, W. J.; Hehre, W. J.; Binkley, J. S.; Gordon, M. S.; DeFrees, D. J.; Pople, J. A. Self-Consistent Molecular Orbital Methods. XXIII. A Polarization-Type Basis Set for Second-Row Elements. *J. Chem. Phys.* **1982**, *77*, 3654–3665.

54. Raghavachari, K.; Trucks, G. W. Highly Correlated Systems. Excitation Energies of First Row Transition Metals Sc–Cu. *J. Chem. Phys.* **1989**, *91*, 1062–1065.

55. Wolinski, K.; Hinton, J. F.; Pulay, P. Efficient Implementation of the Gauge-Independent Atomic Orbital Method for NMR Chemical Shift Calculations. *J. Am. Chem. Soc.* **1990**, *112*, 8251–8260.

56. Adamo, C.; Barone, V. Toward Reliable Density Functional Methods without Adjustable Parameters: The PBE0 Model. *J. Chem. Phys.* **1999**, *110*, 6158–6170.

57. Dunning, T. H. Gaussian Basis Sets for Use in Correlated Molecular Calculations. I. The Atoms Boron through Neon and Hydrogen. *J. Chem. Phys.* **1989**, *90*, 1007–1023.

58. Toomsalu, E.; Burk, P. Critical Test of Some Computational Methods for Prediction of NMR ^{1}H and ^{13}C Chemical Shifts. *J. Mol. Model.* **2015**, *21*, 244.

59. Turnes Palomino, G.; Fisicaro, P.; Bordiga, S.; Zecchina, A.; Giamello, E.; Lamberti, C. Oxidation States of Copper Ions in ZSM-5 Zeolites. A Multitechnique Investigation. *J. Phys. Chem. B* **2000**, *104*, 4064–4073.

60. Schoonheydt, R. A. Transition Metal Ions in Zeolites: Siting and Energetics of Cu^{2+}. *Catal. Rev.* **1993**, *35*, 129–168.

61. Giordanino, F.; Vennestrøm, P. N. R.; Lundegaard, L. F.; Stappen, F. N.; Mossin, S.; Beato, P.; Bordiga, S.; Lamberti, C. Characterization of Cu-Exchanged SSZ-13: a Comparative FTIR, UV-Vis, and EPR Study with Cu-ZSM-5 and Cu-β with Similar Si/Al and Cu/Al Ratios. *Dalton T.* **2013**, *42*, 12741–12761.

62. Teraoka, Y.; Tai, C.; Ogawa, H.; Furukawa, H.; Kagawa, S. Characterization and NO Decomposition Activity of Cu-MFI Zeolite in Relation to Redox Behavior. *Appl. Catal. A-Gen.* **2000**, *200*, 167–176.

63. Oord, R.; Schmidt, J. E.; Weckhuysen, B. M. Methane-to-Methanol Conversion over Zeolite Cu-SSZ-13, and Its Comparison with the Selective Catalytic Reduction of NO_x with NH_3. *Catal. Sci. Technol.* **2018**, *8*, 1028–1038.

64. Markovits, M. A. C.; Jentys, A.; Tromp, M.; Sanchez-Sanchez, M.; Lercher, J. A. Effect of Location and Distribution of Al Sites in ZSM-5 on the Formation of Cu-Oxo Clusters Active for Direct Conversion of Methane to Methanol. *Top. Catal.* **2016**, *59*, 1554–1563.

65. Smeets, P. J.; Hadt, R. G.; Woertink, J. S.; Vanelderen, P.; Schoonheydt, R. A.; Sels, B. F.; Solomon, E. I. Oxygen Precursor to the Reactive Intermediate in Methanol Synthesis by Cu-ZSM-5. *J. Am. Chem. Soc.* **2010**, *132*, 14736–14738.

66. Bosacek, V. Formation of Surface-Bonded Methoxy Groups in the Sorption of Methanol and Methyl Iodide on Zeolite Studied by ^{13}C MAS NMR Spectroscopy. *J. Phys. Chem.* **1993**, *97*, 10732–10737.

67. Blasco, T.; Boronat, M.; Concepcion, P.; Corma, A.; Law, D.; Vidal-Moya, J. A. Carbonylation of Methanol on Metal-Acid Zeolites: Evidence for a Mechanism Involving a Multisite Active Center. *Angew. Chem.-Int. Ed.* **2007**, *46*, 3938–3941.

68. Tsiao, C.; Corbin, D. R.; Dybowski, C. Investigation of Methanol Adsorbed on Zeolite H-ZSM-5 by Carbon-13 NMR Spectrometry. *J. Am. Chem. Soc.* **1990**, *112*, 7140–7144.

69. Salvador, P.; Fripiat, J. J. Molecular Diffusion and Proton Exchange in Methanol Adsorbed by a Sodium and a Hydrogen Y Zeolite. *J. Phys. Chem.* **1975**, *79*, 1842–1849.

70. Park, S.-K.; Kurshev, V.; Luan, Z.; Wee Lee, C.; Kevan, L. Reaction of NO with Copper Ions in Cu(II)-Exchanged ZSM-5 Zeolite: Electron Spin Resonance, Electron Spin Echo Modulation and Fourier Transform Infrared Spectroscopy. *Microporous Mesoporous Mater.* **2000**, *38*, 255–266.

71. Zhao, Z.-J.; Kulkarni, A.; Vilella, L.; Nørskov, J. K.; Studt, F. Theoretical Insights into the Selective Oxidation of Methane to Methanol in Copper-Exchanged Mordenite. *ACS Catal.* **2016**, *6*, 3760–3766.

72. Gabrienko, A. A.; Yashnik, S. A.; Kolganov, A. A.; Sheveleva, A. M.; Arzumanov, S. S.; Fedin, M. V.; Tuna, F.; Stepanov, A. G. Methane Activation on H-ZSM-5 Zeolite with Low Copper Loading. The Nature of Active Sites and Intermediates Identified with the Combination of Spectroscopic Methods. *Inorg. Chem.* **2020**, *59*, 2037–2050.

TOC Graphic

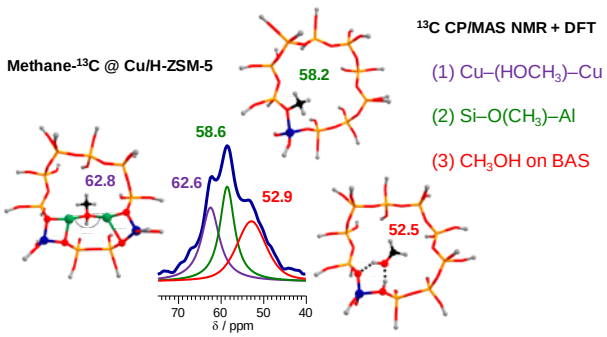

Supporting information

The Nature of the Surface Intermediates Formed from Methane on Cu-ZSM-5 Zeolite: A Combined Solid-State NMR and DFT Study

Alexander A. Kolganov,[1] *Anton A. Gabrienko,*[1,2] *Svetlana A. Yashnik,*[1]

Evgeny A. Pidko,[3,*] *Alexander G. Stepanov*[1,2,*]

[1]Boreskov Institute of Catalysis, Siberian Branch of the Russian Academy of Sciences, Prospekt Akademika Lavrentieva 5, Novosibirsk 630090, Russia

[2]Faculty of Natural Sciences, Department of Physical Chemistry, Novosibirsk State University, Pirogova Str. 2, Novosibirsk 630090, Russia

[3]Inorganic Systems Engineering group, Department of Chemical Engineering, Faculty of Applied Sciences, Delft University of Technology, Van der Maasweg 9, Delft 2629 HZ, The Netherlands

*e-mail: E.A.Pidko@tudelft.nl; stepanov@catalysis.ru

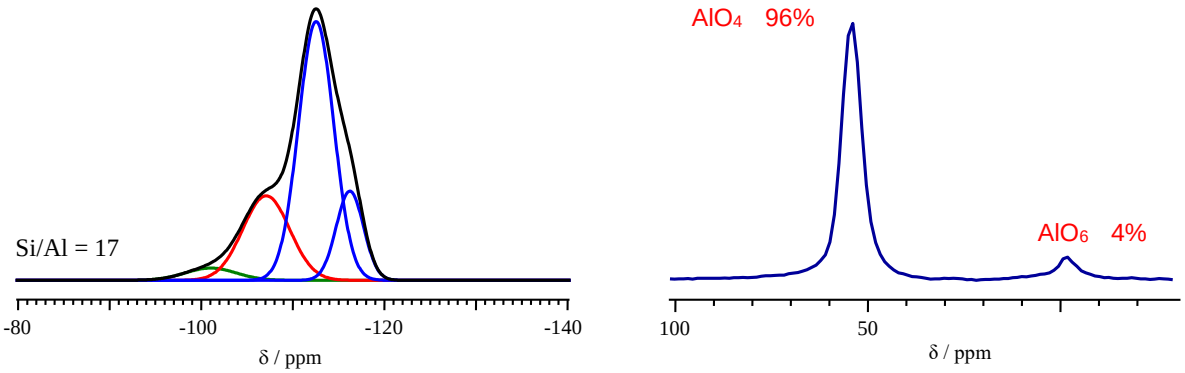

Figure S1. ^{29}Si MAS NMR (left) and ^{27}Al MAS NMR (right) spectra of parent H-ZSM-5 zeolite.

^{29}Si MAS NMR spectra shows few signals which are exhibited by Q^4(0Al) structural units of ZSM-5 framework (blue lines), Q^4(1Al) structural units of silicon atoms with one aluminum atom in outer coordination sphere (red line), and Q^3(0Al) structural units (green line). The integrated intensities of the signals provide Si/Al ratio of 17 for the zeolite sample according to equation V.6 in ref.[1] ^{27}Al MAS NMR spectrum of the zeolite show the presence of the signals at around 54 and 0 ppm from framework AlO_4 units and extra-framework AlO_6 aluminum species, respectively.[1]

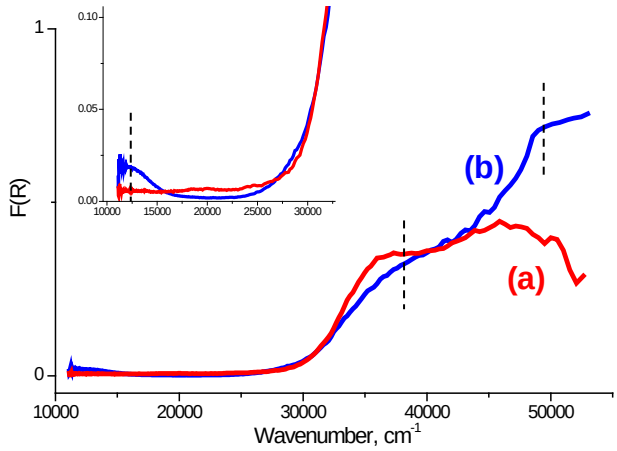

Figure S2. UV–vis DR spectra of parent H-ZSM-5 zeolite (a) and Cu(0.1)/H-ZSM-5 zeolite (b), both at ambient conditions.

Figure S2 shows UV–vis DR spectrum of parent H-ZSM-5 zeolite in comparison with that for as-prepared Cu(0.1)/H-ZSM-5 sample to demonstrate that the adsorption seen at >38000 cm^{-1} is due to the fundamental absorption edge (FAE) of ZSM-5 zeolite.

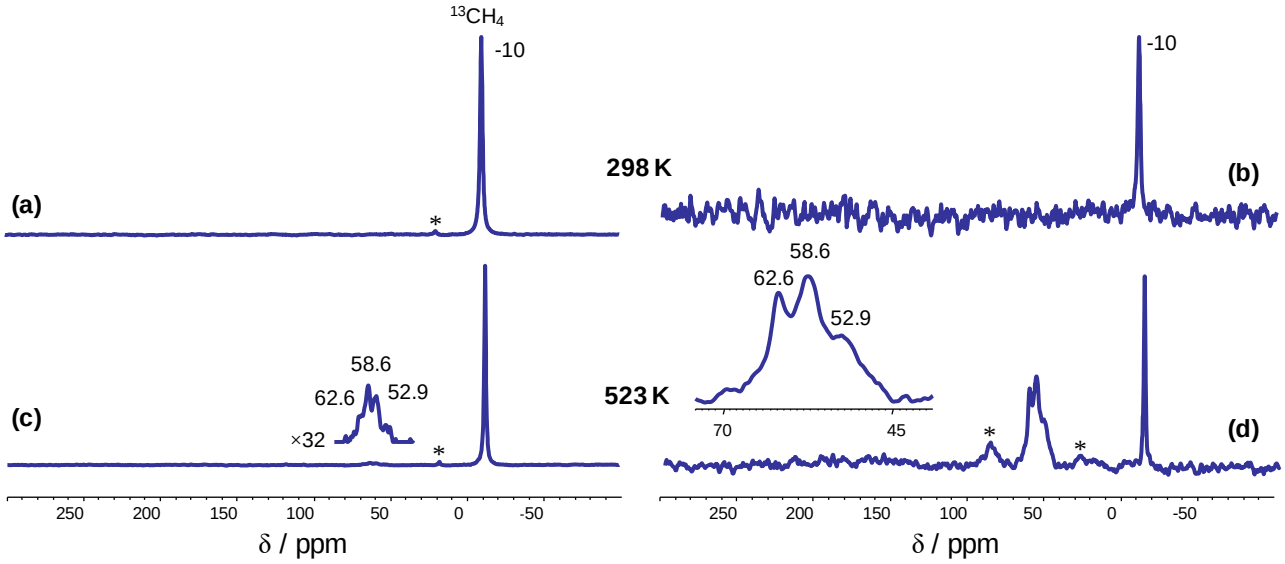

Figure S3. ^{13}C MAS NMR (a,c) and ^{13}C CP/MAS NMR (b,d) spectra of methane-^{13}C adsorbed on dehydrated and O_2 treated Cu(1.4)/H-ZSM-5 at ambient temperature (a, b), and after heating the sample for 1 h at 523 (c, d). Asterisks denote spinning side bands.

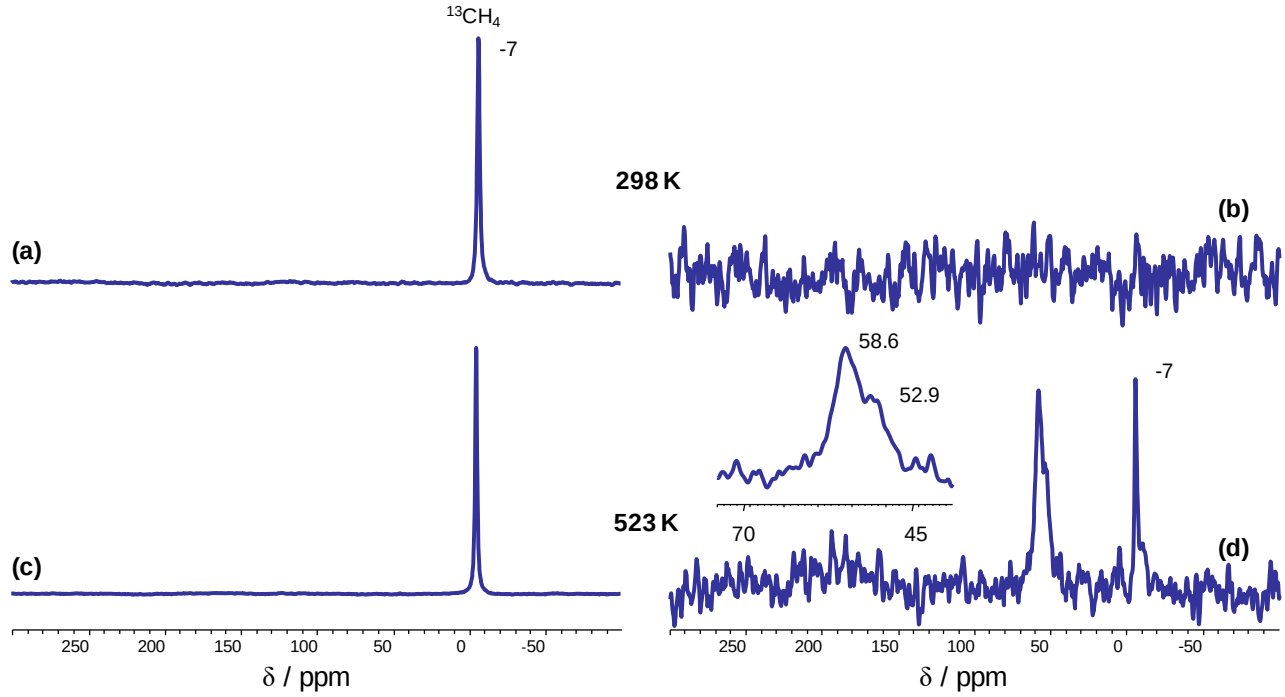

Figure S4. ^{13}C MAS NMR (a,c) and ^{13}C CP/MAS NMR (b,d) spectra of methane-^{13}C adsorbed on dehydrated and O_2 treated Cu(0.1)/H-ZSM-5 at ambient temperature (a, b), and after heating the sample for 1 h at 523 (c, d).

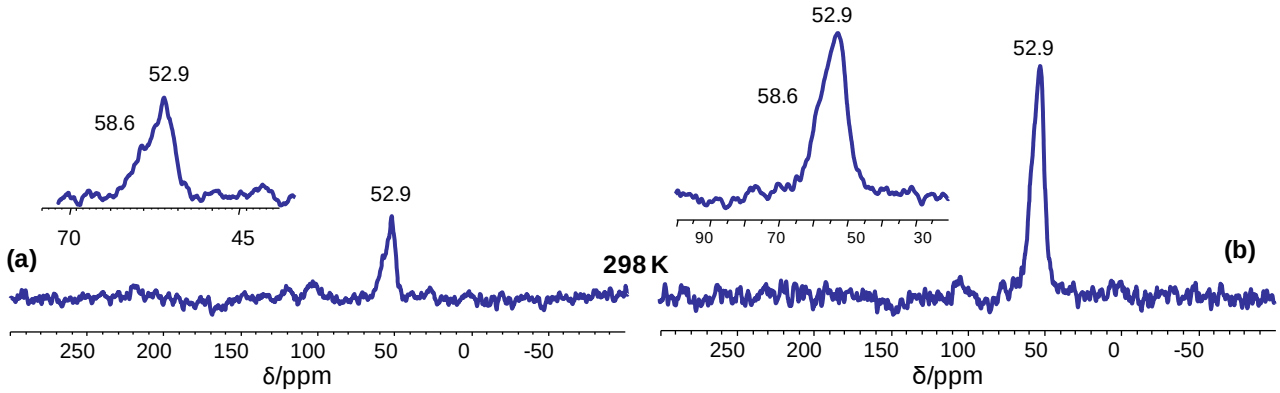

Figure S5. ^{13}C MAS NMR (a) and ^{13}C CP/MAS NMR (b) spectra of methanol-^{13}C adsorbed on dehydrated Cu(1.4)/H-ZSM-5 at ambient temperature.

References

1. Engelhardt, G.; Michel, D., *High-Resolution Solid-State NMR of Silicates and Zeolites*. J.Wiley & Sons: Chichester, 1987; p 150.